

Table of contents

Volume 367

2018

◀ Previous issue Next issue ▶

The 5th International Conference on Advanced Materials Sciences and Technology (ICAMST 2017) 19–20 September 2017, Makassar, Indonesia

Accepted papers received: 16 May 2018

Published online: 12 June 2018

Open all abstracts

Preface

OPEN ACCESS 011001

The 5th International Conference on Advanced Materials Sciences and Technology (ICAMST 2017)

+ Open abstract  View article  PDF

OPEN ACCESS 011002

The List of Committee ICAMST 2017

+ Open abstract  View article  PDF

OPEN ACCESS 011003

List of Participant ICAMST 2017

+ Open abstract  View article  PDF

OPEN ACCESS 011004

Photographs


+ Open abstract  View article  PDF

OPEN ACCESS 011005

Peer review statement

+ Open abstract  View article  PDF

Papers

OPEN ACCESS 012001
This site uses cookies. By continuing to use this site you agree to our use of cookies. To find out more, see our Privacy and Cookies policy. 

A First-principles Investigation of The Adsorption of CO and NO Molecules on Germanene

M. R. Al Fauzan, W. D. Astuti, G. Al Fauzan and Sholihun

[+ Open abstract](#) [View article](#) [PDF](#)

OPEN ACCESS

012052

Synthesis and Characterization Hierarchical Three-Dimensional TiO₂ Structure via Hydrothermal Method

N. Syuhada, B Yulianto and Nugraha

[+ Open abstract](#) [View article](#) [PDF](#)

OPEN ACCESS

012053

Monofilament Wire Silver Sheathed Bi,Pb-Sr-Ca-Cu-O Prepared by Four-Pass Rolling and Repeated Heating Process

Hendrik, P. Sebleku, S. Herbirowo, S. D. Yudanto, B. Siswayanti, Lusiana, H. Nugraha, A. Imaduddin and A. W. Pramono

[+ Open abstract](#) [View article](#) [PDF](#)

OPEN ACCESS

012054

Modified Working Electrode by Magnetite Nanocomposite for Electrochemical Sensor Application

R. N. Suhanto, R. Rahmawati, D. A. Setyorini, I. Noviandri, Suyatman and B Yulianto

[+ Open abstract](#) [View article](#) [PDF](#)

OPEN ACCESS

012055

Effect of Temperature and Duration of Sintering on Perovskite Material (La_{1-x}Ag_x)_{0.8}Ca_{0.2}MnO₃

B. Kurniawan, S. D. Rosanti, R. Kamila, N. B. Sahara, D. S. Razaq, T. Komala and D. R. Munazat

[+ Open abstract](#) [View article](#) [PDF](#)

OPEN ACCESS

012056

Effects of Molar Ratios and Sintering Times on Crystal Structures and Surface Morphology of Nd_{1+x}FeO₃ Oxide Alloy Prepared by using Solid Reaction Method

E. H. Sujiono, J. Agus, S. Samnur and K. Triyana

[+ Open abstract](#) [View article](#) [PDF](#)

OPEN ACCESS

012057

Influence of PT Vale's Granulated Gradation Nickel Slag Aggregate on Compressive Strength of Concrete

E. H. Sujiono, V. Zharvan, S. N. Yunita and S. Samnur

[+ Open abstract](#) [View article](#) [PDF](#)

This site uses cookies. By continuing to use this site you agree to our use of cookies. To find out more,

[OPEN ACCESS](#) and Cookies policy.

012058



PAPER • OPEN ACCESS

Effects of Molar Ratios and Sintering Times on Crystal Structures and Surface Morphology of $\text{Nd}_{1+x}\text{FeO}_3$ Oxide Alloy Prepared by using Solid Reaction Method

To cite this article: E. H. Sujiono *et al* 2018 *IOP Conf. Ser.: Mater. Sci. Eng.* **367** 012056

View the [article online](#) for updates and enhancements.

Related content

- [The Effect of Molar Ratio on Crystal Structure and Morphology of \$\text{Nd}_{1+x}\text{FeO}_3\$ \(\$X=0.1, 0.2, \text{ and } 0.3\$ \) Oxide Alloy Material Synthesized by Solid State Reaction Method](#)
V Zharvan, Y N I Kamaruddin, S Samnur et al.
- [Effect of Molar Ratio on Crystal Structure and Surface Morphology of \$\text{Nd}_1\(\text{Fe}\)_x\text{Ba}_{2-x}\text{Cu}_3\text{O}_7\$ Oxide Alloy by Solid-State Reaction Method](#)
N. A. Humairah, D. Sartika, Muris et al.
- [Influence of High Sintering Temperature Variation on Crystal Structure and Morphology of \$\text{Nd}_{1.2}\text{FeO}_3\$ Oxide Alloy Material by Solid-State Reaction Method](#)
E. H. Sujiono, R. A. Imran, M. Y. Dahlan et al.



IOP | ebooks™

Bringing you innovative digital publishing with leading voices to create your essential collection of books in STEM research.

Start exploring the collection - download the first chapter of every title for free.

Effects of Molar Ratios and Sintering Times on Crystal Structures and Surface Morphology of $\text{Nd}_{1+x}\text{FeO}_3$ Oxide Alloy Prepared by using Solid Reaction Method

E. H. Sujiono¹, J. Agus¹, S. Samnur¹ and K. Triyana²

¹Laboratory of Materials Physics, Department of Physics, Universitas Negeri Makassar, Parang Tambung campus, Makassar 90224, Indonesia

²Department of Physics, Universitas Gadjah Mada, Sekip Utara BLS 21 Yogyakarta 55281, Indonesia

E-mail: e.h.sujiono@unm.ac.id

Abstract. The effects of molar ratios and sintering times on crystal structures and surface morphology on NdFeO_3 oxide alloy have been studied. NdFeO_3 oxide alloy formed by chemical preparation with solid reaction method using raw oxide Fe_2O_3 (99.9 %) and Nd_2O_3 (99.9 %) powders. In this article we reported the effects of molar ratios $x = (-0.1, -0.2$ and $-0.3)$ and sintering times for 15 h and 20 h on crystal structures and surface morphology of $\text{Nd}_{1+x}\text{FeO}_3$ synthesized by solid-state reaction method. The results indicate that variation of molar ratio and sintering time has influenced the FWHM, crystalline size and grain size. The $\text{Nd}_{1+x}\text{FeO}_3$ have a major phase is NdFeO_3 , and other minor phases are Fe_2O_3 , Nd_2O_3 and $\text{Nd}(\text{OH})_3$. The dominant intensity of hkl (121) with a value in FWHM, crystallite size, and grain size an indication the results will be applied as a gas sensor material as the focus of the further study.

Keywords. Crystal structure, $\text{Nd}_{1+x}\text{FeO}_3$, molar ratio, sintering time, surface morphology, and solid state reaction method.

1. Introduction

Metal particles smaller than 100 nm in primary particle diameter are generally considered as nanoparticles. Such metal nanoparticles often exhibit very interesting electronic, magnetic, optical, and chemical properties [1]. For example, their high surface-to-volume ratios have large fractions of metal atoms at surface available for catalysis [2, 3]. The phase majority of catalysts used in modern the chemical industry is based on mixed metal oxides including perovskite oxides ABO_3 [4]. The nano-perovskite oxides ABO_3 (A : La, Nd, Sm, and Gd; B : Fe, Co and Ni; and O : oxygen) have high catalytic activities and high sensitivity with CO and HCs. Their applications in gas sensors were studied especially for its properties in electrical and response for CO gas [5]. NdFeO_3 is a perovskite transition metal oxide with an orthorhombic structure and space group of Pbnm possesses insulator properties at room temperature [6].

One of NdFeO_3 synthesis method is solid reaction method [7]. Solid reaction method is the synthesis of solid materials by reacting with another solid at high temperatures [8]. Solid reaction method is having advantages such as the resulting crystals having good purity and crystallized.



However, the synthesis results obtained in this method produce particles of a large size and irregular morphology [9]. Based on the interesting phenomena developing of oxide materials using the solid-state method, the authors have the conduct of previous research for fabrication oxide material such as $\text{YBa}_2\text{Cu}_3\text{O}_y$, $\text{NdBa}_2\text{Cu}_3\text{O}_y$, $\text{NdFe}_x\text{Ba}_{2-x}\text{Cu}_3\text{O}_y$ and $\text{Nd}_{1+x}\text{FeO}_3$, the results have been reported elsewhere [10–14].

In this study will be assessed the effect of molar ratio and sintering time on crystalline structure and surface morphology of $\text{Nd}_{1+x}\text{FeO}_3$ prepared by solid-state reaction method. Heating temperature, heating time and molar ratio are important because it can be adjusted to crystallinity, grain size, and homogeneity. Therefore, the development of NdFeO_3 oxide material needs to be realized to obtain the best crystal structure and surface morphology for gas sensor application.

2. Materials and methods

Preparation of $\text{Nd}_{1+x}\text{FeO}_3$ material was made 6 samples, 3 samples with a variation of molar ratio indicate with sample #1, #2 and #3, and 3 samples with a variation of sintering time indicate with sample #4, #5 and #6. In this study, $\text{Nd}_{1+x}\text{FeO}_3$ oxide Alloy Material were synthesized from Nd_2O_3 (99.9 %) and Fe_2O_3 (99.9 %) powder using solid state reaction method. Stoichiometric calculation of raw material mass used Proust law with molar ratio value are $x = -0.1$, $x = -0.2$ and $x = -0.3$ for sample #1, #2 and #3, respectively and $x = 0$ for sample #4, #5 and #6. The mixed was grinded by mortar and pastel for ± 3 hours to maximize the reaction and then were calcined using the furnace. The sample #1, #2 and #3 was calcined at 950°C for 50 h, sample #6 at 600°C for 40 h. Sample #4 and #5 without calcination process. After calcination process is complete, the sample then prepared into a pellet with 1.25 cm diameter under 16 t pressure. The pellet of sample #1, #2 and #3 then sintered at temperature 950°C for 67 h, sample #4 and #6 at 400°C for 20 h and sample 5 at 400°C for 15. All of the samples were characterized using XRD to identify the crystalline phase and using SEM to identify the surface morphology.

3. Results and discussion

3.1. Variation of molar ratio

3.1.1. Chemical Composition

The spectrum showed that increased of peaks intensity and widened of peaks width when the value of the molar ratio is added. However, there are some irregularities where the intensity of the peak sample #2 ($x = -0.2$) higher than sample #1 ($x = -0.1$) at certain positions.

Figure 1 shows the addition of the molar ratio, the peak intensity continues to increase, and the peak width becomes wider. However, there are some deviations in which the intensity of the peak $x = -0.2$ is higher than $x = -0.1$ at certain positions, e.g., at 32.6° corresponding to the hkl (121). The XRD characterization result obtained that the sintering temperature influence of the FWHM. The FWHM is 0.11° for the sample #1, related to the intensity of 984.56 counts. The similar results have been reported on reference [2, 4, 11, 14] though with different research method.

The crystals size of NdFeO_3 was calculated on the basis of Scherrer's equation at the highest peak and obtained the crystals size from the smallest to the largest is associated with $x = -0.2$ (94.0 nm), $x = -0.1$ (109.7 nm) and $x = -0.3$ (131.6 nm). While XRD diffraction pattern obtained of FWHM value for molar ratio varied of $x = -0.1$, $x = -0.2$ and $x = 0$, at 32.6° corresponding to the hkl (121) are 0.11° , 0.13° and 0.12° and the intensity for each molar ratio is 834 counts, 979 counts and 474 counts, respectively.

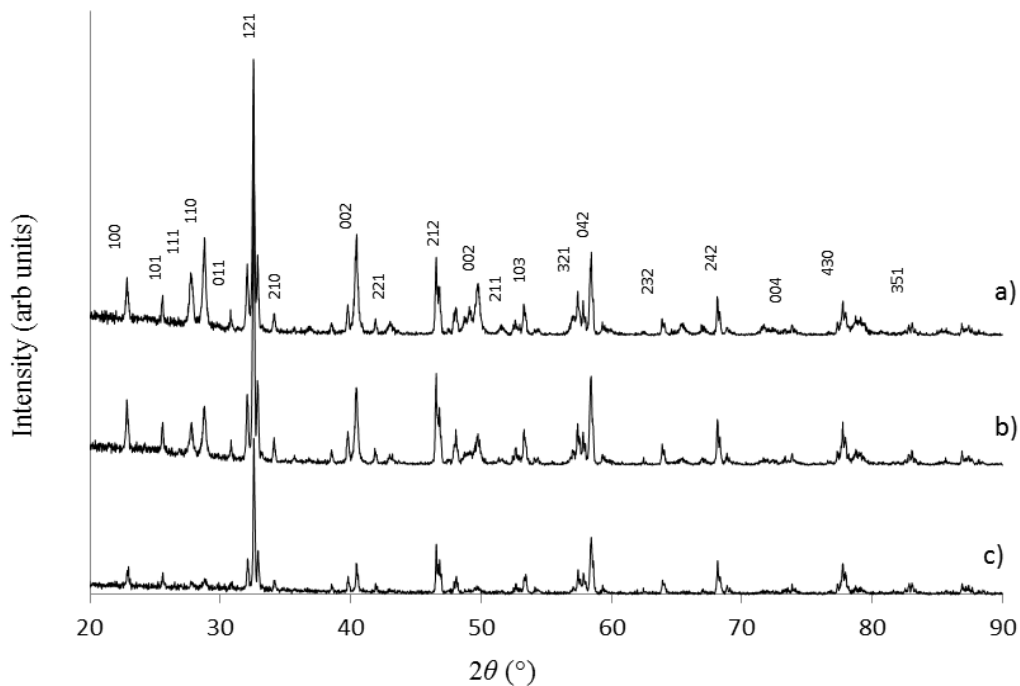


Figure 1. XRD spectra of a) sample #1 , b) sample #2 and c) sample #3, respectively.

3.1.2. Microstructure and Microanalysis

Figure 2 shown SEM image of the $\text{Nd}_{1+x}\text{FeO}_3$ alloy was prepared with different parameter process. As shown in the figure, it can be seen that the morphology in Figure 2.a and Figure 2.b is more homogeneous although there are still grain boundaries. This data indicated that the result from phase composition was obtained is confirmed. On the other hand, based on Figure 2.c shows that many of grain size shape were observed and this is caused by appearing of grain boundaries. Therefore, we confirmed that the sintering temperature also has influence formed of grain size and grain boundary [3, 9, 11]. Based on the SEM image of the samples above, the variation of the molar ratio has a clumpy surface morphology in which the grain boundary appears on the sample looks very thin and is almost invisible, and the crystalline grain appears much unified.

Crystalline phases analysis using the software *Match!* shows each sample contains four phases is NdFeO_3 , $\text{Nd}(\text{OH})_3$, Fe_2O_3 and Nd_2O_3 . It can be seen in Table 1, increasing of molar ratio gradually increase the percentage of NdFeO_3 phase. Similar results have been reported in previous studied [13], and there is a minority phase of $\text{Nd}(\text{OH})_3$ due to the absorption of hydrogen and oxygen by neodymium [15].

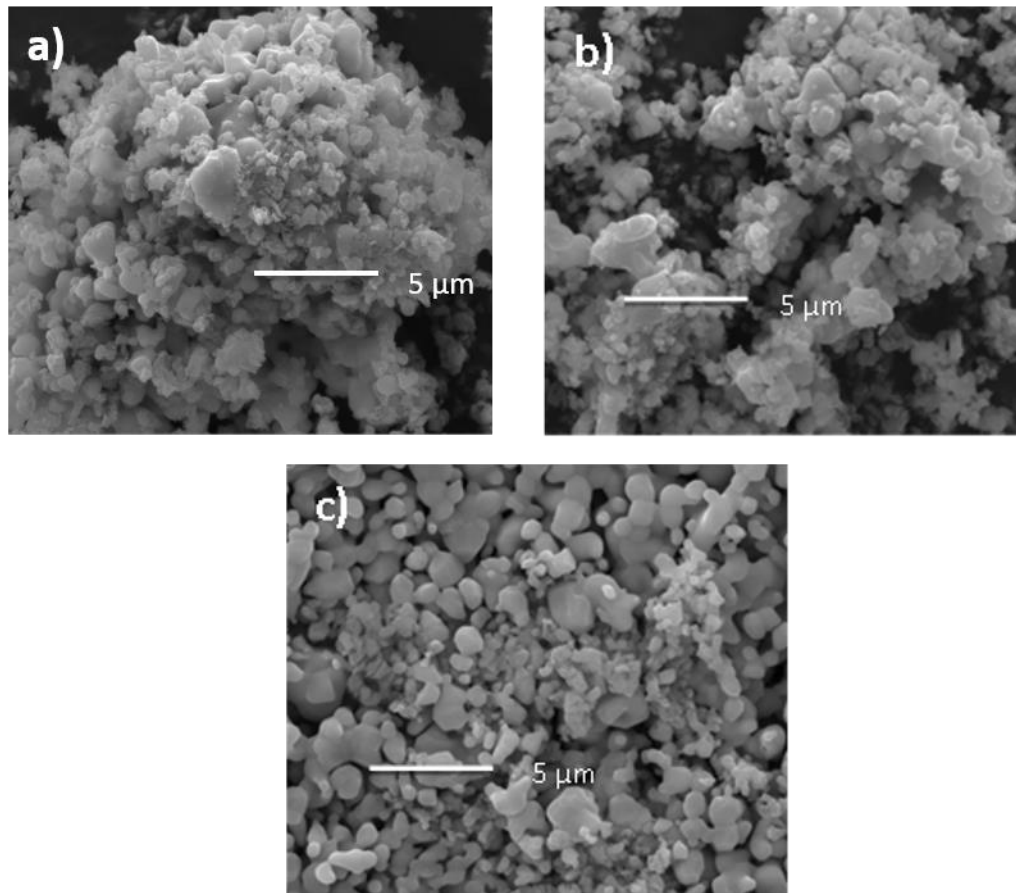


Figure 2. SEM images of a) sample #1, b) sample #2 and c) sample #3 with mag. of 20,000x.

Table 1. Phase analysis of the $\text{Nd}_{1+x}\text{FeO}_3$ samples.

Samples	NdFeO_3 (%)	Nd_2O_3 (%)	Fe_2O_3 (%)	$\text{Nd}(\text{OH})_3$ (%)
#1	83	4	-	13
#2	83	4	5	8
#3	78	4	7	11

3.2. Variation of sintering times

3.2.1. Chemical Composition

The XRD graph shown in Figure 3, it is can be seen that if $\text{Nd}(\text{OH})_3$ phase formed almost dominant, in contrast, that the oxide alloy material has not formed NdFeO_3 phase. It can be seen clearly that there are many peaks with a variation of intensity value as shown in Figure 3.a sample #4 and Figure 3.b sample #5. These results also confirmed that the synthesis process does not show the formation of NdFeO_3 phase. However, based on the results of sample #5 the oxide alloy material still forms the $\text{Nd}(\text{OH})_3$ phase, although the sintering time is 5 h longer than sample #4 which is sintered for 15 h. This structure can also be seen that the most dominant peak as an indication of NdFeO_3 phase still does not observe as consequences of the sintering process at a low temperature of 400 °C and without calcination. In contrast Figure 3.c sample #6 show the formation of NdFeO_3 phase indicate the appearance of a peak at 32.6° corresponding to the hkl (121). In fact, this result confirmed of a strong indication that calcination process at 600 °C for 40 h following sintering process at a low temperature of 400 °C still produce oxide alloy with NdFeO_3 phase. It means the calcination process has the more dominant effect of the crystal structure if compare than the sintering time at low temperature.

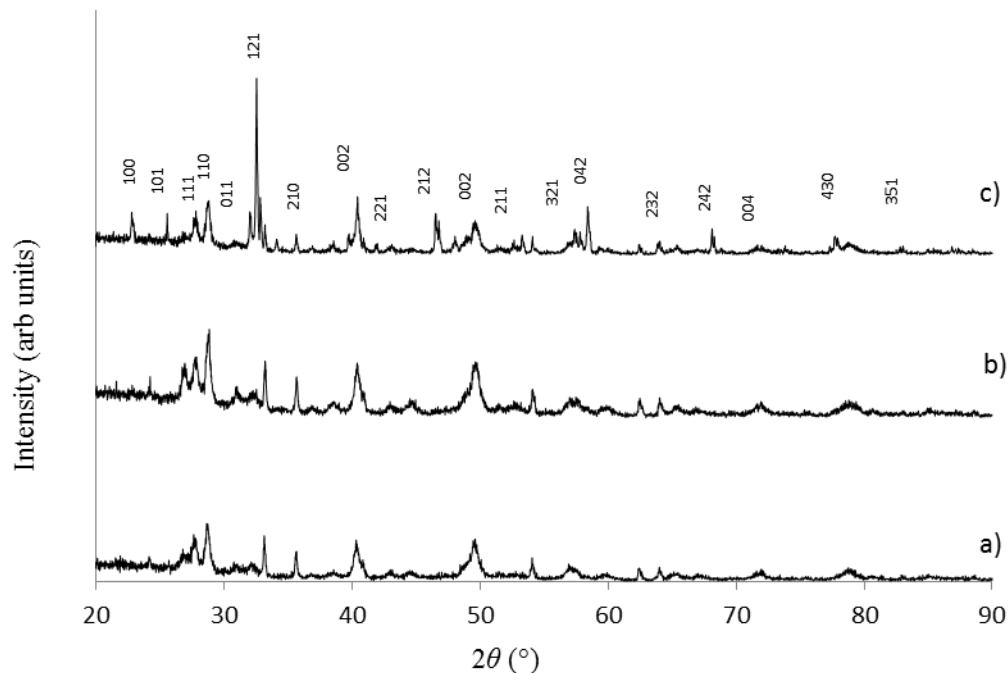


Figure 3. XRD spectra of a) sample #4, b) sample #5 and c) sample #6, respectively.

Calculation of grain size using Debye-Scherrer's equation on the highest intensity obtained crystalline size value are (163.97 ± 0.01) nm, (167.21 ± 0.01) nm and (255.47 ± 0.01) nm for the sample#4, sample #5, and sample #6, respectively. While based on XRD diffraction pattern obtained FWHM value at 2θ of 32.6° for sample #4, sample#5 and sample #6 are 0.19° , 0.19° and 0.12° and the intensity for each sample are 57 counts, 76 counts, and 1227 counts, respectively. This result is similar as has reported by Lou Xiangdong et al. with temperature 800°C [8], Yabin Wang et al. with temperature 1000°C [9] and they get similar results that phase NdFeO_3 exist at $2\theta = 32.56^\circ$ with hkl value is (121). V. Zharvan *et al.* [13] reported the crystalline size of samples ranging at 137.0 – 152.0 nm.

3.2.2. Microstructure and Microanalysis

The SEM image of $\text{Nd}_{1+x}\text{FeO}_3$ samples was shown in Figure 4. It can be seen that all of the samples have non-homogeneous morphology. There are still many agglomerates made due to temperature and mechanical treatment.

Figure 4.a sample #4 and Figure 4.b sample #5 shows an unfinished grain growth forming of NdFeO_3 oxide alloy. Correspond to the crystal structure as have been explained, the surface morphology of the sample #4 and sample #5 indicate with granular patterns that are very difficult to identify. Given the variation of sintering time in these two samples, it does not show any significant difference grain size. However, if we observe more closely at Figure 4.b sample #5, there are some parts that have formed a grain. In contrast, the surface morphology of the sample#6 as shown in Figure 4.c which was calcined for 40 h at a temperature of 400°C then sintered for 20 h at a temperature of 600°C indicates a better morphology than the two samples which is sample #4 and sample #5 without calcination process. The size of the grains is large and in some parts of the surface appear grain growth is not perfect due to the low sintering and calcination temperature. Similiar results were obtained by Khorasani-Motlagh M. *et al.* that synthesis nanocrystals NdFeO_3 materials with has good porosity and the crystalline size influence of time and temperature heat treatment [16].

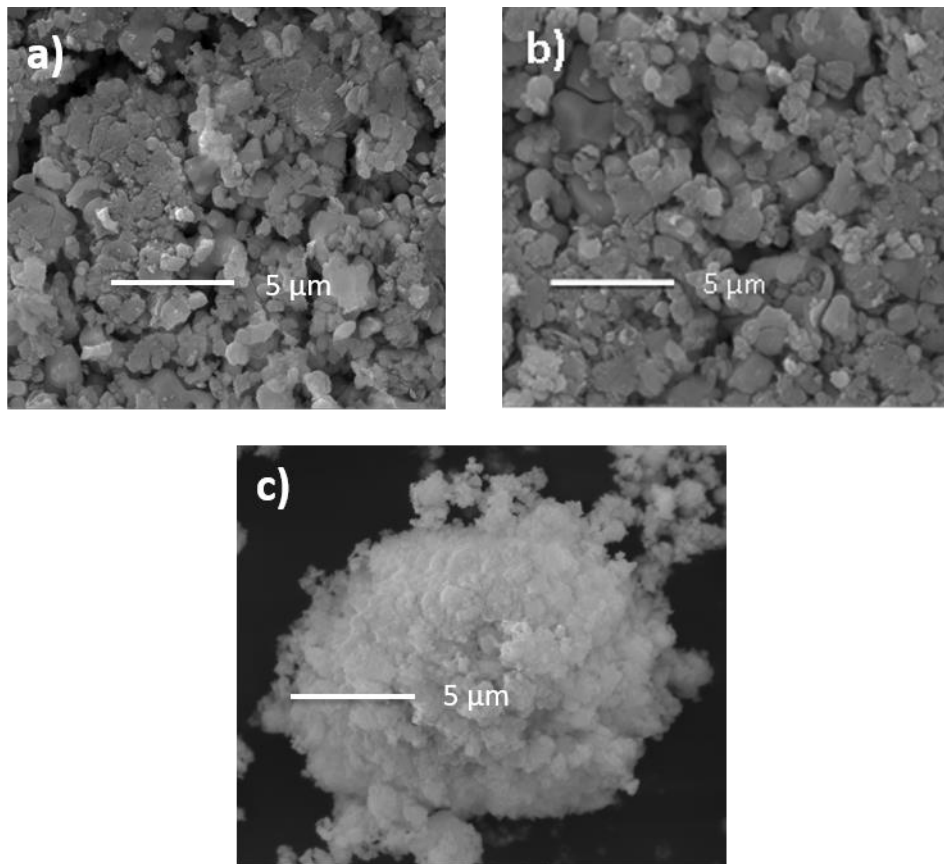


Figure 4. SEM image of a) sample #4, b) sample #5 and c) sample #6 with mag. of 20.000x.

Phases analysis using the software *Match!* show dominant phases of NdFeO_3 and contains phase in each sample are $\text{Nd}(\text{OH})_3$, Fe_2O_3 and Nd_2O_3 , respectively. The highest intensity corresponds to the NdFeO_3 phase with polycrystalline material and orthorhombic structure.

Table 2. Phase analysis of the $\text{Nd}_{1+x}\text{FeO}_3$ samples.

Samples	NdFeO_3 (%)	Nd_2O_3 (%)	Fe_2O_3 (%)	$\text{Nd}(\text{OH})_3$ (%)
#4	55	8	20	17
#5	53	9	19	17
#6	74	2	14	10

It can be seen in Table 1 and Table 2, the percentage of $\text{Nd}(\text{OH})_3$ are quite large due to the absorption of hydrogen and oxygen by neodymium [15]. Its means to produce high quality of NdFeO_3 oxide alloy the temperature of calcination and sintering process for synthesis should be higher than $950\text{ }^\circ\text{C}$ or increasing the heating time that the reaction of the raw material occurs perfectly and containing lattice -OH has missing.

4. Conclusions

The molar ratio greatly affects the crystal structure of $\text{Nd}_{1+x}\text{FeO}_3$ oxide alloy, which is indicated intensity differences, FWHM value, and crystal size. The XRD analyzed was obtained FWHM value is 0.11, 0.13, 0.12, 0.19, 0.19 and 0.12, and crystalline size value of NdFeO_3 are (294.86 ± 0.01) nm, (248.30 ± 0.01) nm, (288.17 ± 0.01) nm, (163.97 ± 0.01) nm, (167.21 ± 0.01) nm and (255.47 ± 0.01) nm for sample #1, #2, #3, #4, #5 and #6, respectively. There are four phases that contain each sample:

NdFeO₃, Nd(OH)₃, Fe₂O₃ and Nd₂O₃. The highest intensity of NdFeO₃ giving information that samples are a polycrystalline material with dominant phase formed is orthorhombic correspond to *hkl* (121).

Acknowledgements

This research was funded by Directorate Research and Community Services, Directorate General of Research and Development, Ministry of Research, Technology, and Higher Education, Republic of Indonesia, under research scheme of *Hibah Kompetensi* fiscal year 2016/2017.

References

- [1] Masoud Salavati-Niasari, Fatemeh Davar and Maryam Shaterian 2008 Preparation of cobalt nanoparticles from [bis(salicylidene)cobalt(II)]-oleylamine complex by thermal decomposition *Journal of Magnetism and Magnetic Materials* **320** 3-4 pp 575–578
- [2] Siegel R. W, Nastasi M, Parkin D. M and Gleiter H. 1993 Synthesis and properties of nanophase materials *Materials Science and Engineering*. **168** (2) pp 189–197
- [3] Siegel R W 1994 Nanostructured materials –mind over matter *Nanostructured Materials* **4** (1) pp 121–138
- [4] Pena M A and Fierro J L G 2001 *Chem. Rev* **101** (7) pp 1981–2018
- [5] Truong G H *et al* 2011 *Adv. Nat. Sci: Nanosci. Nanotechnol* **2** p 015012
- [6] Anhua W *et al* 2009 Preparation of ReFeO₃ nanocrystalline powders by auto-combustion of citric acid gel *Asia-Pac. J. Che. Eng.* **4** pp 518–521.
- [7] Yabin W *et al* 2011 Growth rate dependence of the NdFeO₃ single crystal grown by float-zone technique *Journal of Crystal Growth* **318** pp 927–931
- [8] Truong Giang Ho 2011 Nanosized perovskite oxide NdFeO₃ as material for a carbon-monoxide catalytic gas sensor *Advances In Natural Sciences: Nanoscience And Nanotechnology* **2** p 015012
- [9] Xiangdong Lou, X Jia, and J Xu 2005 *Journal of Rare Earths* **23** (3) pp 328–331
- [10] Sujiono E H 2017 ID Patent No. P00200800471 Reg. No. 44179
- [11] Sujiono E H *et al* 2001 Crystal Structure and Morphology Analysis of Nd_{1+x}Ba_{2-x}Cu₃O₇ Oxide Alloy Surface Developed by Solid State Reaction Method *Physica Status Solidi (A) Applied Research* **187** pp 471–479.
- [12] Sujiono E H, Arifin P and Barmawi M 2002 YBa₂Cu₃O_{7-δ} thin films deposited by a vertical MOCVD reactor *Materials Chemistry and Physics* **73** pp 47–50.
- [13] V. Zharvan *et al* 2017 The Effect of Molar Ratio on Crystal Structure and Morphology of Nd_{1+x}FeO₃ (X=0.1, 0.2, and 0.3) Oxide Alloy Material Synthesized by Solid State Reaction Method *IOP Conference: Materials Science and Engineering* **202** pp 012072
- [14] Sujiono E H *et al* 2011 *Jurnal Teknologi dan Aplikasi (ITS)* **7** pp 166–173
- [15] Pedro V S *et al* 2016 *Materials Research* **19** (2) pp 389–393
- [16] Khorasani-Motlagh M *et al* 2013 Chemical Synthesis and Characterization of Perovskite NdFeO₃ Nanocrystals via a Co-Precipitation Method *Int. J. Nanosci. Nanotechnol* **9** (1) pp 7–14
- [17] Xinshu N *et al* 2003 *Journal of Rare Earth* **21** (6) pp 630–632
- [18] Ru Zhang *et al* 2010 Electrical and CO-sensing properties of NdFe_{1-x}Co_xO₃ perovskite system *Journal of Rare Earths* **28** (4) pp 591–595
- [19] Shujuan Y *et al* 2011 The magnetic properties and specific heat of NdFeO₃ single crystal were systematically studied in the temperature range from 2 to 300 K *Journal of Applied Physics* **109** p 07E141
- [20] Zhang *et al* 2009 Lanthanide hydroxide nanorods and their thermal decomposition to lanthanide oxide nanorods *Materials chemistry and physics* **114** (1) pp 160-167